Available online at www.sciencedirect.com

SCIENCE DIRECT®

Journal of Volcanology and Geothermal Research 146 (2005) 226–240

Journal of volcanology and geothermal research

www.elsevier.com/locate/jvolgeores

Geological aspects of the 2003–2004 eruption of Anatahan Volcano, Northern Mariana Islands

Setsuya Nakada[a,*], Takeshi Matsushima[b], Mitsuhiro Yoshimoto[a], Takeshi Sugimoto[b], Teruyuki Kato[a], Tsuyoshi Watanabe[c], Ramon Chong[d], Juan T. Camacho[d]

[a]*Earthquake Research Institute, University of Tokyo, Yayoi, Bunkyo-ku, Tokyo 113-0032, Japan*
[b]*Institute of Seismology and Volcanology, Kyushu University, Shimabara 855-0843, Japan*
[c]*Faculty of Science, Kochi University, Kochi 780-8520, Japan*
[d]*Emergency Management Office, P.O. Box 501704 CK, Saipan MP 96950, Northern Mariana Islands*

Received 31 July 2004; accepted 24 October 2004

Abstract

Anatahan Volcano, Northern Mariana Islands, began erupting in May–June 2003. A series of subplinian explosive eruptions of andesite magma began at the Eastern Crater in the eastern part of the summit caldera on the evening of 10 May. Brown tephra was sent mainly westward by strong winds. Small-scale pyroclastic surges were discharged eastward outside the caldera in late May. An andesite lava dome that had once filled the inner crater was fragmented by phreatomagmatic explosions in the middle of June. The phreatomagmatic explosions probably occurred due to interaction of the magma head with groundwater around the crater, and abundant very fine ash ("gray tephra") was discharged within the caldera and over most of the island. The volume of eruption products of the May–June eruption was estimated to be 1.4×10^7 m^3 dense-rock-equivalent. Erupted pumices and lava are aphyric andesite and are variously colored depending on their vesicularity. The SiO_2 contents of erupted materials decreased slightly with time. The fine gray ash is depleted in alkalies, probably due to leaching by acid hydrothermal fluids during explosions. Seismic activity resumed in late March 2004, and small strombolian-like explosions were repeated in May and June 2004. About half of the inner crater was filled with new scoria and lava.

Keywords: Anatahan; phreatomagmatic eruption; tephra; infrared image; eruption volume

1. Introduction and previous activity

Anatahan Volcano is located at the southern end of the emergent Northern Mariana volcanic chain (Fig. 1a). Anatahan is about 9 km long in the east–west direction and about 4 km wide in the north–south direction. Anatahan island is the uppermost portion of

* Corresponding author. Fax: +81 3 3812 6979.
E-mail address: nakada@eri.u-tokyo.ac.jp (S. Nakada).

0377-0273/$ - see front matter © 2005 Elsevier B.V. All rights reserved.
doi:10.1016/j.jvolgeores.2004.10.023

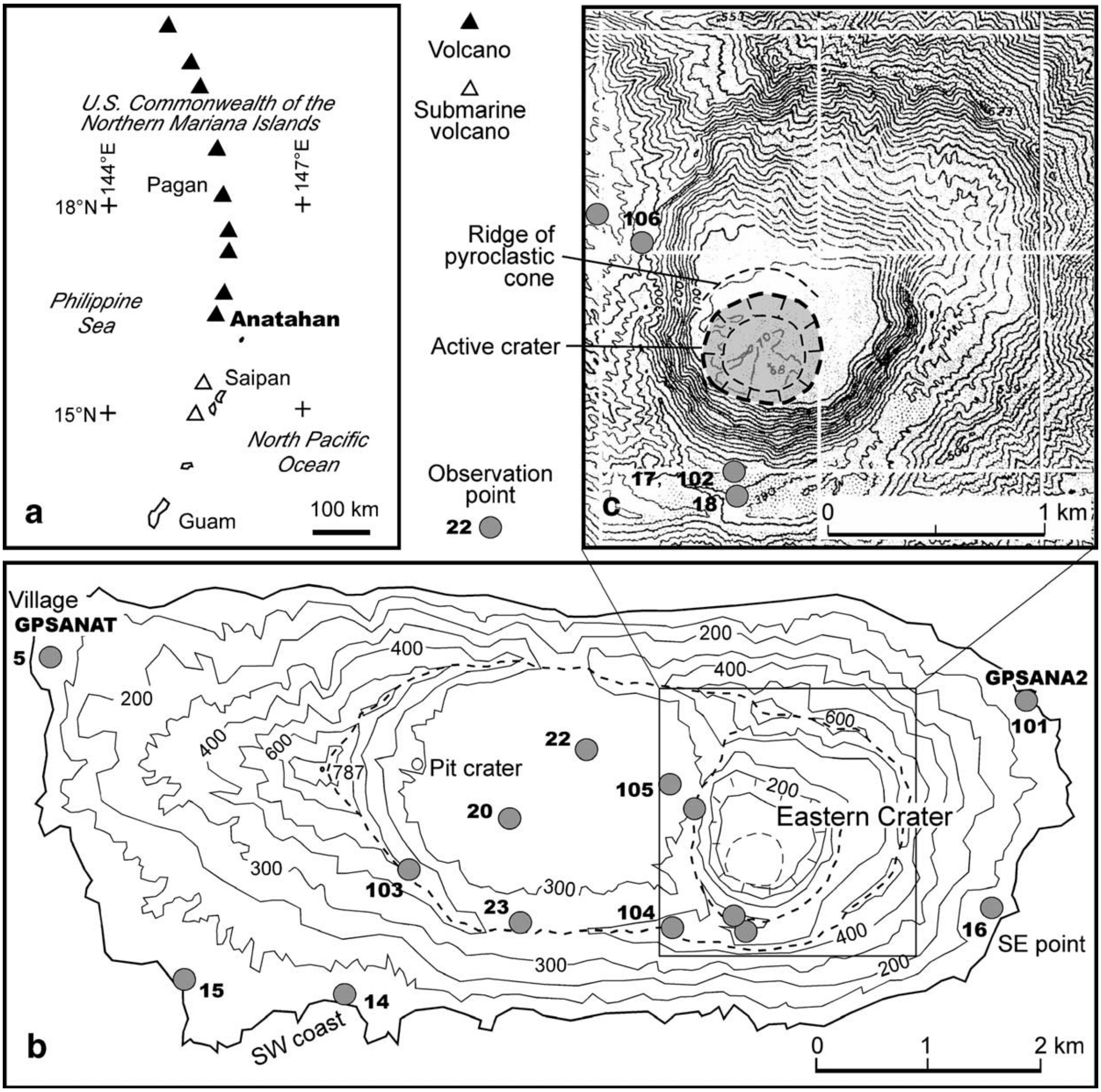

Fig. 1. Index maps of Anatahan Volcano. a) Distribution of active volcanoes in the North Mariana Islands. b) Topographic map of Anatahan, showing observation points with location numbers and a pit crater with the most recent morphology. GPSANAT and GPSANA2 are GPS observation stations (Watanabe et al., 2005—this issue). c) Detailed topographic map of the Eastern Crater, where the present active center is outlined. From Sheet #3371 IIISE, series W843, US Army Map Service.

a big stratovolcano that stands on the sea bottom as deep as 2,000 m with a diameter of up to 15 km, according to bathymetry maps by Johnson (2003). A large east–west elongated caldera 6 km long by 3 km wide occupies an area covering about half of the island (Fig. 1b). The floor of the western part of the caldera is flat, containing the morphology showing several large craters filled with young deposits. The eastern part is mostly occupied by a large crater, Eastern Crater (Fig. 1c). The floor of the Eastern Crater was 68 m above sea level (asl) before the 2003 eruption. The origin of the caldera is unknown.

Accumulation of pyroclastic surge layers up to a few tens of meters thick can be observed in the uppermost part of the caldera walls and is also extensive outside the caldera. The caldera may have resulted from drainage of magma from the magma reservoir beneath the summit by submarine eruption or dike intrusion under the sea, such as the 1968 eruption of Fernandina Volcano, Galapagos (Simkin and Howard, 1970) or the 2000 eruption of Miyakejima Volcano, Japan (Nakada et al., in press). The distribution of basalt and dacite volcanic rocks from Anatahan Volcano was reported by Tanakadate (1940), Larson et al. (1975) and Woodhead (1988).

No volcanic activity before the May 2003 event has been documented. Rowland and Lockwood (1990) reported hydrothermal activity on the floor of the Eastern Crater and the existence of a non-eroded pit crater, and they suggested that Anatahan may have erupted in very recent time. One crater may have existed with steaming within the caldera during and after World War II. Maruyama (1954) showed an illustration of a volcanic crater with a rising plume in the southern part of a great basin jungle together with hot springs in the eastern smaller basin. The great and small basins probably represent the western part of the summit caldera and the Eastern Crater, respectively. In fact, a topographically very young crater a few tens of meters across is located at the western periphery of the caldera (pit crater in Fig. 1b), although the exact location is a little different from the place in the illustration. Strong earthquake swarms occurred under Anatahan in 1990 and 1993, and all islanders were forced to move off the island in May 1993 (Sako et al., 1995).

The 2003 eruption began around 1700 local time on May 10 (e.g., Bulletin of Gobal Volcanism Network, hereafter BGVN, v. 28, nos. 4, 5 and 6; Wiens et al., 2004). An eruption cloud rose as high as 13.4 km on May 10 and the height subsequently decreased (4600 m on 11 May, 2400 m on 12 May according to Trusdell et al., 2005—this issue). On 23–24 May the wind direction changed from the usual westerly direction to southeasterly, due to the approach of a typhoon, so that falling ash was reported in Saipan and Guam more than 100 km south of Anatahan. A spiny surface of a lava dome was first observed within the vent on 4 June. Seismic activity increased after 12 June, and strong explosions, which were believed to have removed most parts of new lava dome, were observed on 14 June. Darker clouds rose on 16 June. Eruptive activity declined after the explosions of middle June 2003. Following elevated seismic activity in late March of 2004, less-energetic explosive activity than in the May–June 2003 eruption started and continued to at least July 2004 (BGVN v.29, no. 4).

Correlation of the eruption sequence with eruption products is not clear, though some results of field observation were briefly reported by D. Hilton and T. Fischer (BGVN v. 28, no. 5). We carried out a geological inspection of the active crater and eruption products as part of a GPS campaign observation (Kato et al., 2003), in July 2003, January and June 2004, in order to understand the eruption processes from a geologic point of view and to evaluate the potential for future eruptions. In this paper, we describe the eruption and the geologic aspects of the eruption products.

2. Crater activity

2.1. 18–19 July 2003

An inner crater about 300 to 400 m across, slightly elongated in a northwest–southeast direction, was active on the floor of the Eastern Crater adjacent to the southern wall. Weak white steam was rising from the bottom and walls of the inner crater (Fig. 2b). Visibility was obscured by a drifting plume of discolored volcanic gas. A strong smell of SO_2 was present on the southern ridge of the Eastern Crater and its abundance in air was measured at slightly over 5 ppm by the portable gas detector. The bottom of the inner crater was filled with mud and water, considered to have poured from the surrounding steep walls. There are three main drainages into the inner crater: southwest, northeast and southeast. Observation with an infrared camera (AVIO Neothermo TVS-620) on the crater rim and in a helicopter showed that the hottest spot (about 300 °C) was located at the upper part of the northern wall of the inner crater (Fig. 3a1). The outline of the inner crater was not circular; a mound with a rugged surface covered with thin deposits was located in the northeastern corner of the crater. Although this might have been a part of

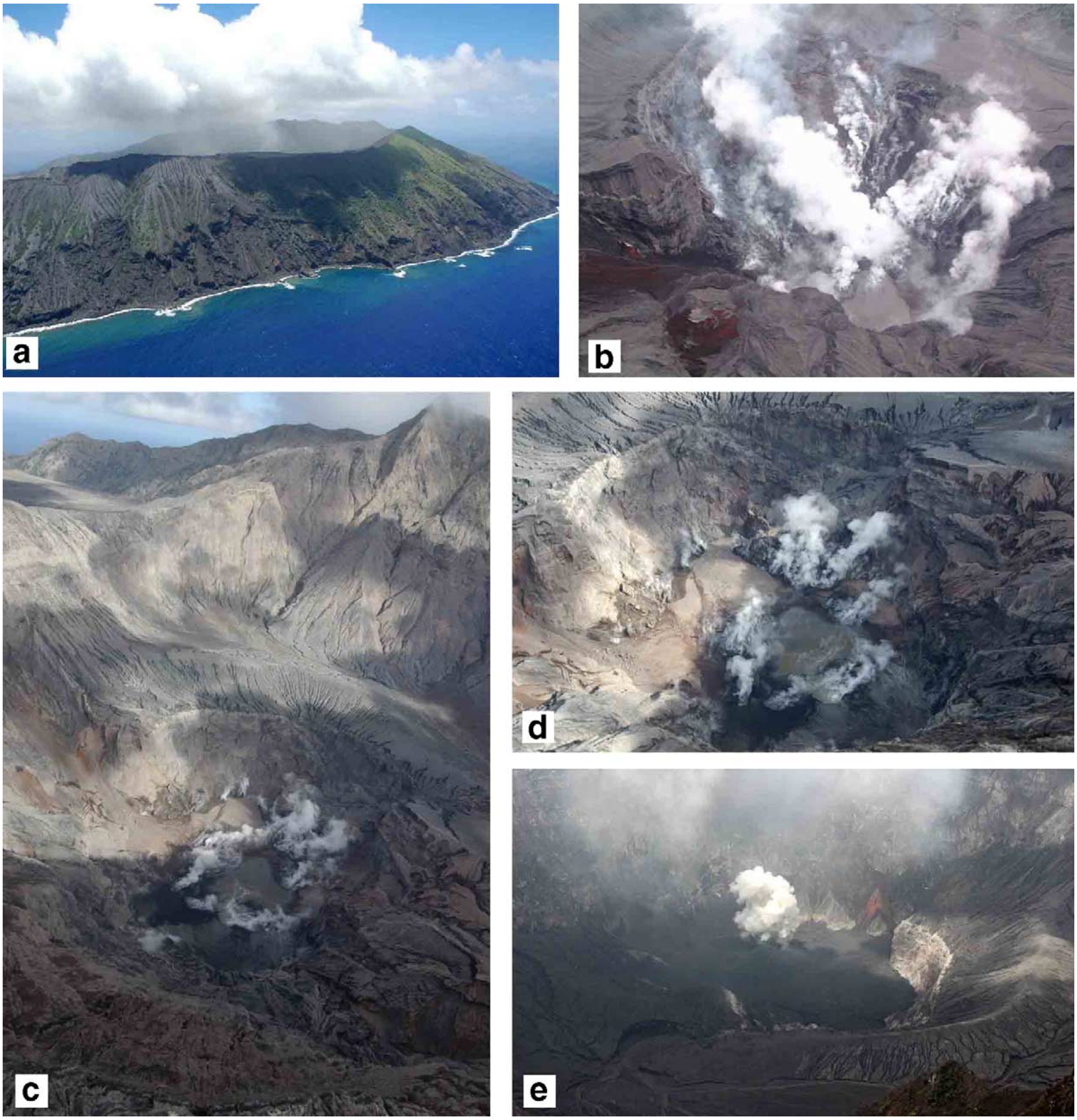

Fig. 2. Photographs of the Eastern Crater of Anatahan Volcano. a) Southerly view of the eastern part of the Anatahan island, taken on 11 June 2004. b) Inner crater in the Eastern Crater, seen from the southeast on 19 July 2003. c) and d) Southeasterly view of the inner crater and the Eastern Crater on 26 January 2004. e) Northerly view of the erupting inner crater on 11 June 2004. a and e by TM, b–d by SN.

lava dome that appeared in early June and was fragmented during the middle June explosions, the surface temperature was not high in the infrared image (fore side of Fig. 3a1). There is a curved ridge outside the inner crater in the northern part, which looks like part of a shallow-sided pyroclastic cone (Figs. 1c and 2c, e). This ridge existed even before the May–June eruption as shown in a photograph taken in 1999 (not shown here). This may be a part of a tuff cone formed during a prehistoric eruption.

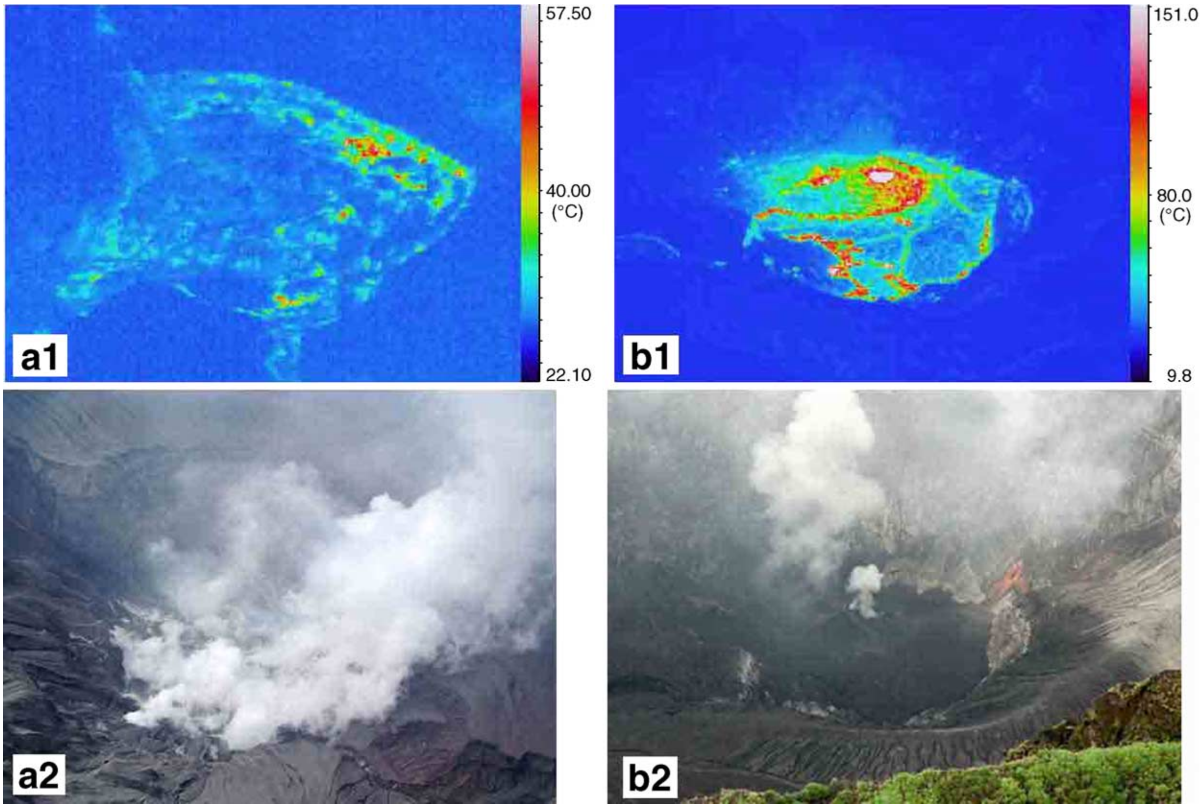

Fig. 3. IR- and real images of the inner crater. a) Easterly view on 19 July 2003. b) Northerly view on 11 June 2004.

A section of new deposits as thick as 15–20 m and thinning outward was observed in the upper part of the inner crater walls (Fig. 2b). Blocks repeatedly discharged during the eruption (BGVN v. 28, nos. 4 and 5) were not observed on the surface of the deposits within the Eastern Crater. It is likely that they penetrated into the soft deposits and were covered by later deposits.

2.2. 25–26 January 2004

Since July 2003, the inner crater was slightly enlarged by spalling of rocks from the walls, and shallowed by deposition of mud on the crater floor. The amount of gas and steam had greatly decreased so that visibility was better than in middle July 2003 (Fig. 2c and d). Dimensions of the inner crater were measured from the southern rim of the Eastern Crater using a laser distance meter (NEC LX3200), field compass, alidade, and hand-held GPS. The inner crater is roughly circular about 400 m across and 80 m deep (Fig. 1c). The altitude of the crater bottom is 15–20 m asl. Comparing photographs from the same angle taken in July 2003 and January 2004, the crater bottom is about 30 m deeper in July 2003 than in January 2004. Therefore, the crater bottom likely was below sea level shortly after the June 2003 eruption. A mass of angular lava blocks emitting white steam was observed in the northeast corner of the inner crater floor (Fig. 2d). These are remnants of a mound that had survived collapse of the northeastern corner of the inner crater floor in July 2003. A temperature of 150 °C was observed in spaces between lava blocks. The highest temperature of 151 °C was recorded at a fumaroles located in the western corner of the crater floor. As a whole, the inner crater had cooled down since middle July 2003. The bottom of the active crater was flat, and there were water pools of different sizes, at least two of which were intensively steaming (Fig. 2d). Mud was gushing as high as several meters at intervals of several seconds within the eastern pool, resembling small strombolian explosions.

2.3. 11 June 2004

Seismic activity had been elevated since late March of 2004 and eruption occurred in early April 2004 (BGVN v. 29, nos. 4 and 5). Formation of a new lava dome on the bottom of the inner crater was reported on 16 April, and the explosive stage began on 28 April. In the inspection of 11 June 2004, the inner crater was filled by scoria darker than the usual pumice, and by black lava up to about half the height of the crater wall of January 2004 (Fig. 2e). Two active vents were located in an east–west direction in the south-central part of the crater floor. These locations are close to the hot pools observed in January 2004 (Fig. 2c and d). The explosions, which occurred with a frequency of strombolian activity, were repeated from the western vent at intervals of several seconds. White explosion clouds rose less than 200 m above the vent. Bombs discharged by these explosions, less than 1 m across, were scattered around the vent. Incandescence was observed at the base of the rising cloud soon after explosions, and when large bombs broken open upon hitting the ground. The eastern vent discharged an ash-laden light brown cloud at intervals of several tens of minutes. The ash clouds rose up to about 600 m above the vent. A low and elongated spatter cone, about 300 m long and 200 m wide, was formed around the two vents. In the infrared images (Fig. 3b1), the two vents are highest in temperature and the spatter cones are surrounded by the high temperature zone. Bright dots scattered around the vent are bombs discharged by explosions. The maximum temperature measured with the infrared camera from the helicopter was about 151 °C. A high-temperature zone was also found along crater walls, probably originating from high-temperature fumaroles. Relatively high-temperature lines (80–120 °C) were observed in the flat surface north of the spatter cones, similar to crust boundaries in Hawaiian lava lakes (e.g., Wright et al., 1992). The northern flat surface may represent a lava flow discharged from the active vents that filled the northern part of the crater.

3. Eruption products

3.1. General statement

Gray-colored ash covered most of the island, except the eastern part where green palm trees were visible in middle July 2003. Everywhere inside the caldera was thickly covered by gray ash and standing trees were very scarce (Fig. 4a, b). As commonly observed when fine ash deposited by phreatic to phreatomagmatic eruptions (e.g., the 2000 eruption in Miyakejima Volcano; see Nakada et al., in press), rills and gullies developed extensively around rises and ridges. Small branches on the few standing trees were almost all stripped off, and the surviving trees were coated thickly by gray ash toward the Eastern Crater, implying strong lateral movement of gray ash from the Eastern Crater. Abundant flat bundles of thatch stems were exposed on the bottom of eroded rills, or from the lower sections of deposits eroded by mud flows and water current. This implies that these stems were blown down in the early stage of, or before the gray tephra eruption.

Eruption products of the May–June 2003 eruption consist mainly of lower brown and upper gray tephra, both of which are composed of multiple layers of different colors, grain sizes and abundances of clasts (Figs. 5 and 6). Geologic inspection at the Anatahan village (point 5) on 21 May by Hilton and Fischer (BGVN v.28, no. 5; http://www.margins.wustl.edu/SF/Anatahn/Anatahan20030529.html) showed that the dark brown clast-rich ash layer in the uppermost part of brown tephra (their "mixture of coarser grained ash and angular clasts of scoriaceous material (2 inches)") was the topmost layer of the deposit. In middle July, this layer was covered by fine gray ash (Figs. 5c and 6). As eruption resumed in middle June, the gray ash was considered to be a product of middle June 2003, when eruption clouds higher than 2 km were witnessed (BGVN v. 28, no. 6). The fact that the color of eruption cloud in middle June was dark to light gray, much different from the reddish to light brown colors in the May eruptions, also supports this stratigraphic identification. Erosion was observed everywhere between the brown and gray tephra (Figs. 5c and 6), suggestive of a relatively long hiatus in eruptive activity.

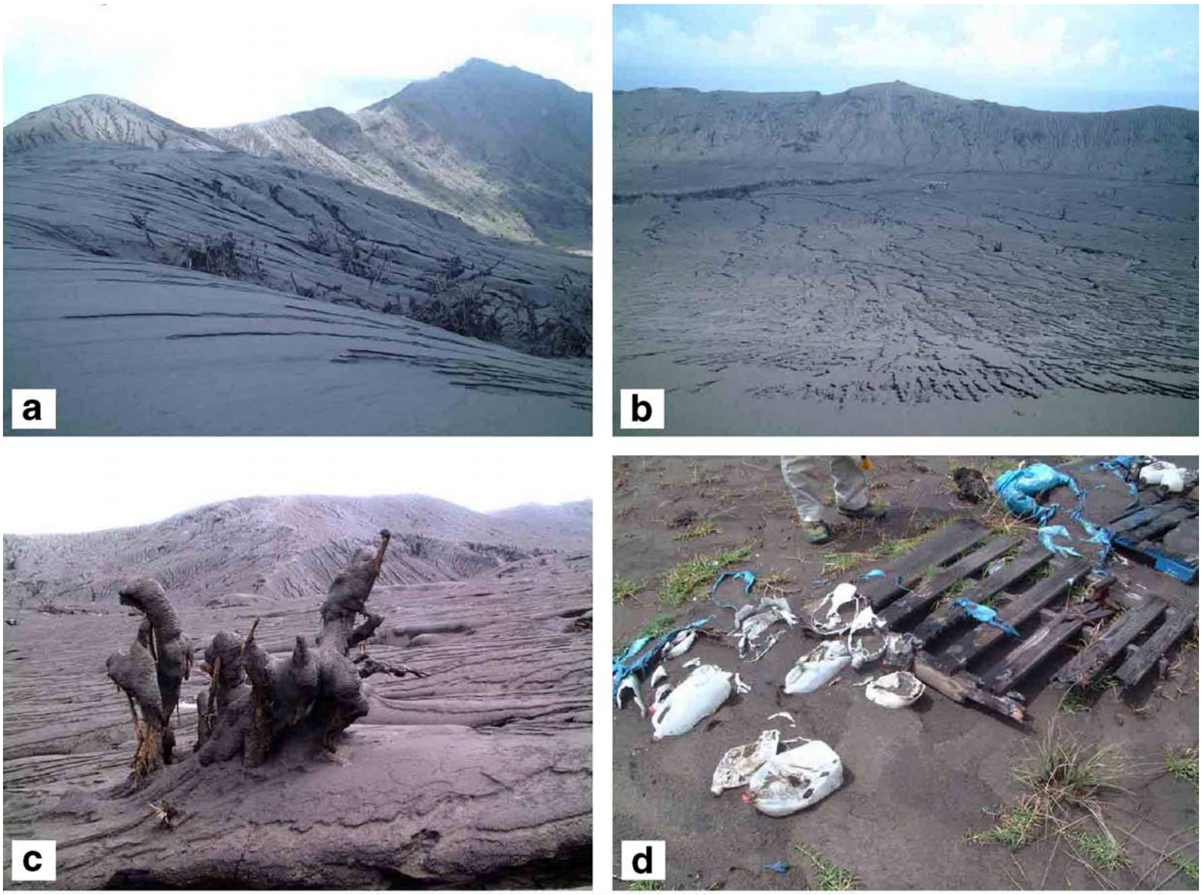

Fig. 4. Photographs showing deposition of tephra in middle July 2003. a) The southern rim of the caldera was thickly covered with gray tephra (near point 23). b) The southern outer-slope of the Eastern Crater and caldera floor were covered completely by gray tephra (seen from point 17). This surface was accessed by helicopter. c) Standing trees on the southern outer-slope of the Eastern Crater, whose branches were taken away, were coated on the crater side by gray ash (between points 18 and 17). d) Partly melted plastic containers within a prehistoric crater in the southeastern end of the island were covered thinly by brown ash (point 16). All photos were taken on 18 and 19 July 2003 by SN.

3.2. Brown tephra

Brown tephra is thick in the eastern part of the Eastern Crater, up to about 15 m thick at the eastern rim of the active crater, with a major axis to the west and a minor axis to the northeast (Fig. 7). It consists of pumice- and ash-fall layers and poorly sorted ash layers of surge or flow origin. Several layers of pumice-fall deposits are observed within the caldera. At point 18, pyroclastic surge deposits directly cover sand and gravel on the previous ground surface (Fig. 6). They are poorly sorted as shown by their grain size distribution (bottom of Fig. 8). Stems of plants in this deposit were partly burnt. A dark brown clast-rich layer is always found in the western part of the crater, and is as thick as 50 cm near the Eastern Crater inside the caldera. Near the Eastern Crater, the dark brown layer occupies more than half of the section of the brown tephra. At point 18, south of the Eastern Crater, dark brown pumice lumps up to about 10 cm across are closely packed. This is considered to be a layer equivalent to the clast-rich ash or lapilli layer inside the caldera and in the western part of the island (Fig. 6). Clasts in brown tephra are vesiculated light-colored pumice or less-vesiculated darker pumice. Accidental altered lava fragments are found commonly in the lowermost thin layer at most observation points. Large pumice clasts are composed of a dark brown, porous

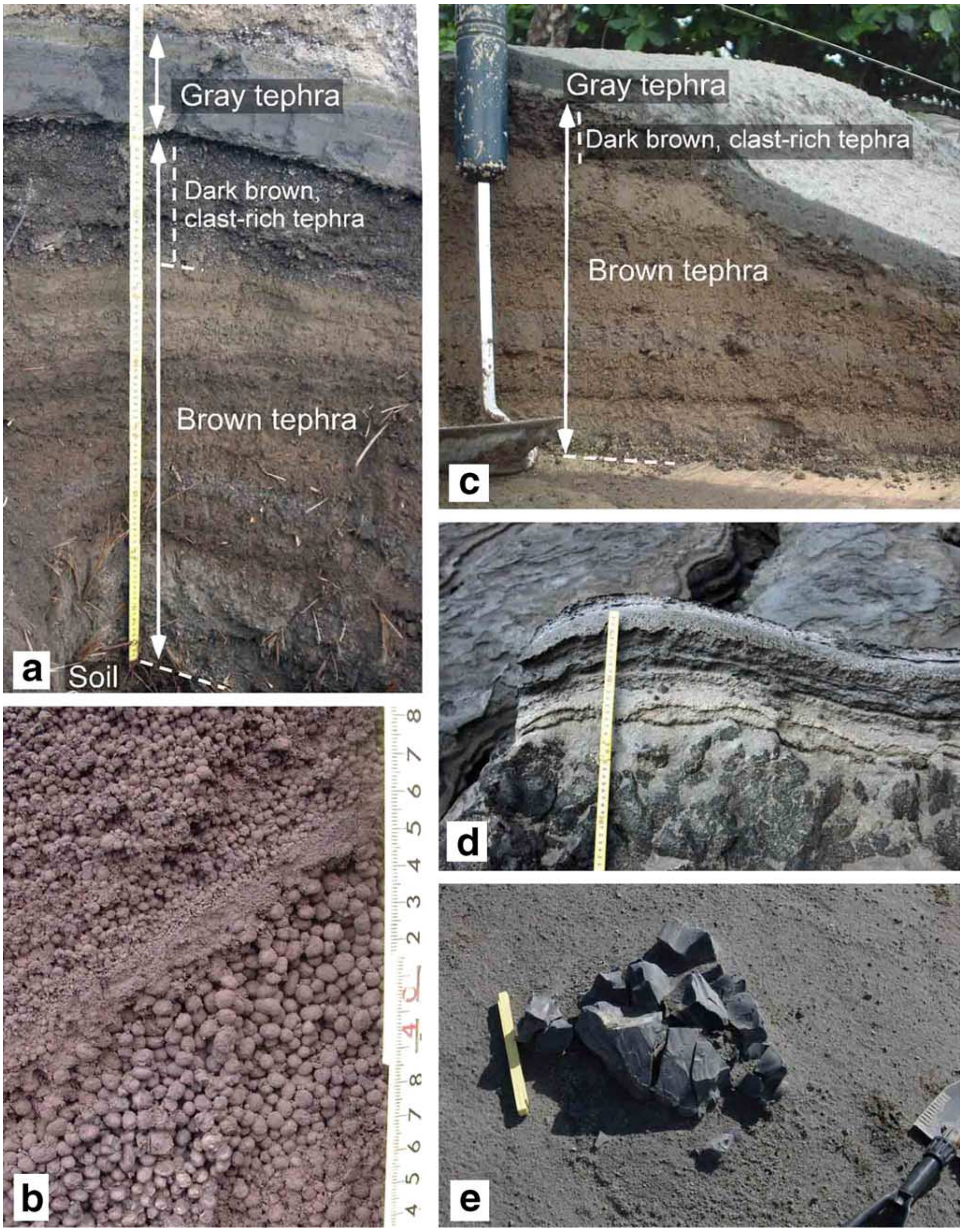

Fig. 5. Photographs showing sections of tephra and deposition of bombs. a) Section of tephra on the southwestern rim of caldera (point 103). Scale in the image is 95 cm long. b) Layers consisting mainly of accretionary lapilli on the southwestern coast (point 14). c) Section of tephra deposited on a table in Anatahan Village (point 5). d) Brownish gray lithic-rich layers on an andesite bomb on the southern outer-slope of the Eastern Crater (between points 18 and 17). Scale bar in the image is 35 cm long. e) Glassy bomb with cooling joints that landed on the top of gray tephra on the western rim of the Eastern Crater (point 106). Scale bar is 20 cm long. Photos a, d, and e on 25–26 January 2004, and b and c on 17–18 July 2003. All by SN.

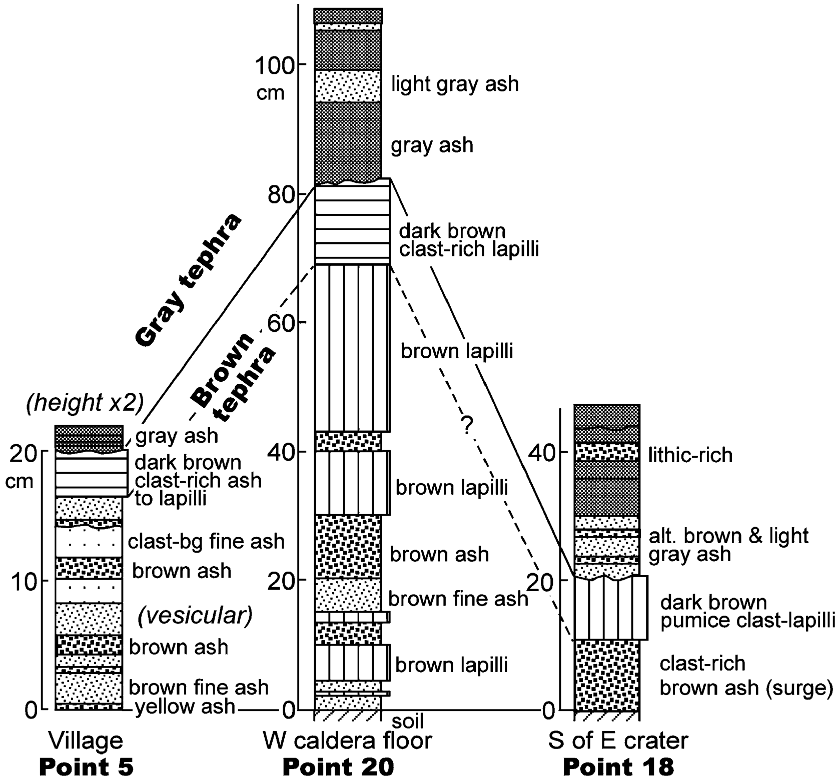

Fig. 6. Geologic sections at three locations (points 5, 20 and 18).

inner core with light-brown, less-vesiculated crust. Vesicularity is variable, up to >60%, even within single clasts and from grain to grain.

Layers consisting mainly of accretionary lapilli, up to 5 mm across, were observed on slopes at the eastern and southern coasts (points 5, 14 and 15) (Fig. 5b). Such aggregations were limited to steep slopes, contrasting with deposits on the flat surfaces, where vesiculated tuff or isolated accretionary lapillies in the ashy matrix were observed. Layers of accretionary lapilli are accumulated successively, where the lapilli are closely packed without ashy matrix, like caviar. Abnormal aggregations of accretionary lapilli on slopes like this may have been formed by rolling and growing up on slopes during deposition, not only by aggregation inside the eruption plume.

3.3. Gray tephra and volcanic bombs

Gray tephra is mainly distributed inside the caldera, along a west–northwest axis (Fig. 7). The lowest rim of the Eastern Crater coincides with the direction of the main axis. Gray tephra is considered to be a product of phreatomagmatic explosions and base surges, because it is composed of very fine ash particles forming distinct and continuous layers as thin as a few cm. It is likely that abundant gray ash was sent through the lowest rim of the Eastern Crater by cock's tail jets with low-angles. It is plausible that gray tephra was discharged by explosions reported as "light-colored, steam-dominated, eruption cloud got darker and rose very quickly" for the 16 June 2003 event (BGVN v.28, no.6, p. 11).

The lowest part of the gray tephra consists of alternating thin layers of dark brown, clast-rich and a gray ash (Fig. 5d; point 18 in Fig. 6). Ash particles of gray tephra are very fine, less than 1 mm across even on the southern rim of the Eastern Crater. Under the microscope, most particles are black in color and rounded in shape, implying that they were quenched glass and worn down due to collision to each other in eruption column. Bimodal distribution seen in grain

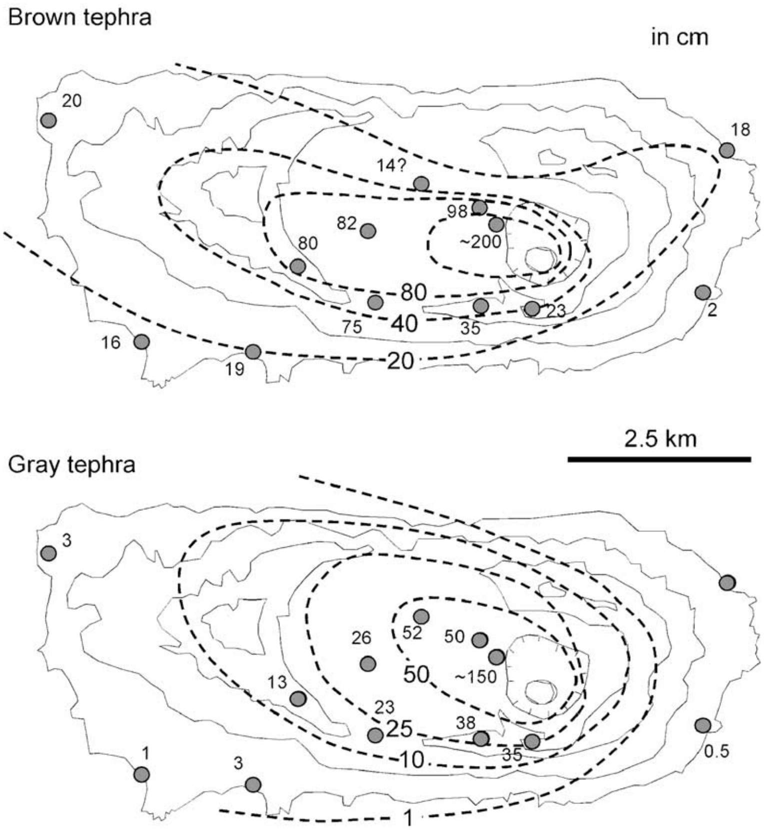

Fig. 7. Isopach maps of brown (lower) and gray tephra (upper) of the 2003 eruption.

size distribution of gray tephra (data for point 17 in Fig. 8) also indicates involvement of accretionary lapilli or aggregation of ash particles in the deposits.

In places close to the Eastern Crater, volcanic bombs up to 1 m across are seen in the gray tephra. Bombs are black in color and their surfaces are quenched and jointed. The bombs are neither recycled older bombs nor older lavas, because they are chemically identical to one another and close to the chemistry of pumice clasts in the brown tephra, as described later. As their occurrence is not limited into a single horizon, the discharge of bombs took place throughout eruption of the gray tephra. For example, a bomb is covered by a layer of the lowermost of gray tephra (Fig. 5d), and a part of another bomb is exposed on the surface of the gray tephra within the crater rim (Fig. 5e). These features suggest that fragmentation of the lava dome began in the early stage of the gray tephra eruption. This suggestion is compatible with the BGVN report (v. 28, no. 6, p. 11) stating that most of lava dome was removed by the 14 June 2003 explosions.

3.4. Ash-cloud surge at the SE point of Anatahan

Although the southeastern point of the island (point 16) was not covered with ash before 19 May 2003, it was later covered thinly with ash, and partially melted plastic containers were found on 6 June (http://hvo.wr.usgs.gov/cnmi/update.html; http://www.margins.wustl.edu/SF/Anatahn/Anatahan2003first.html) (Fig. 4d). It was speculated that an ash cloud hotter than 200 °C swept this area (BVGN v. 28, no. 5). Though the inspection in middle July 2003 did not show any heat effects on plants near the melted containers, a carton box and wooden plate were found partly burnt. Ash as thick as 2.5 cm was deposited on the wooden plate. The deposit consists of both lower gray ash layers and upper brown layers. Brown ash is the

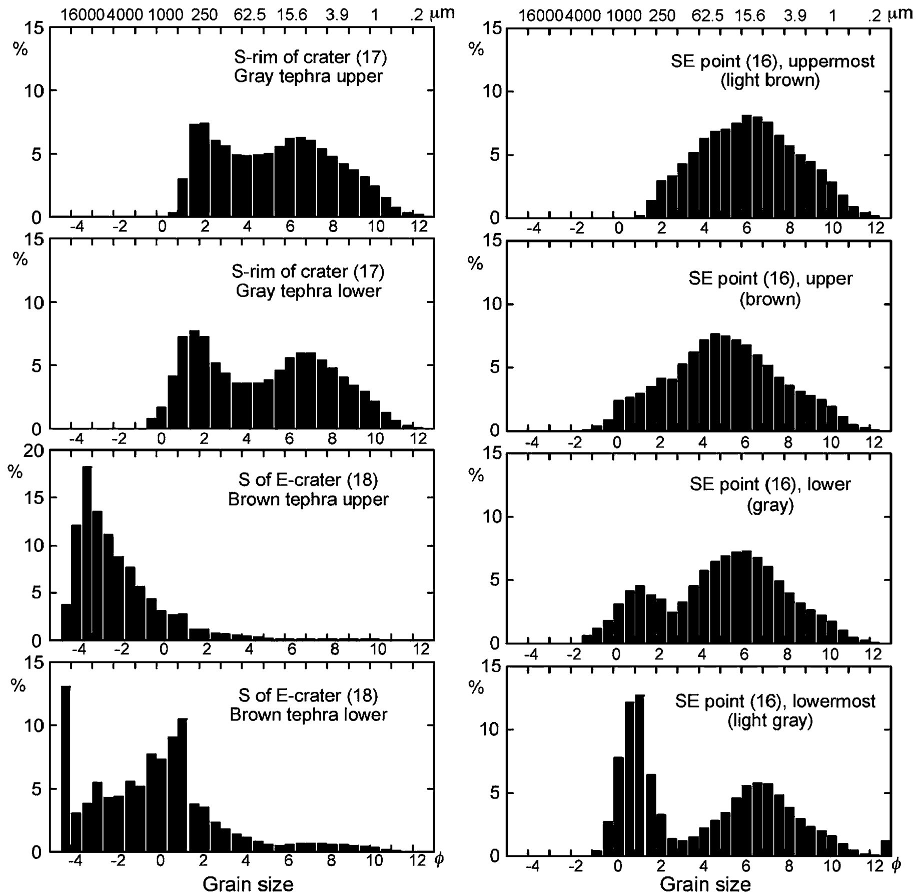

Fig. 8. Grain size distribution of deposits on the southern rim and outer-slope of the Eastern Crater (points 17 and 18) and within a prehistoric crater in the southeastern end of the island (point 16).

candidate for the heat source that partly melted the plastic containers. Grain size distribution patterns shows well-sorted brown ash (two samples from point 16, upper right of Fig. 8), closer to ash-fall than to a pyroclastic flow. However, ash-cloud surge deposits often have sorting that is better than that of ash-fall ashes (Fujii and Nakada, 1999). Probably, gray ash from a phreatic eruption first covered the ground, followed by a high-temperature ash-cloud. The latter flowed down from the crater and expanded upward at this site due to decreasing density, providing heat to partly melt the plastic containers. Plants already covered by ash were unaffected. A similar situation was also found in the 2000 eruption of Miyakejima Volcano, where volcanic bombs discharged during the eruption penetrated into roofs of wooden houses without burning (Nakada et al., in press). A typhoon approached Anatahan on 23 and 24 May 2003, and wind directions changed from westerly to easterly. The isopach map for brown tephra shows a secondary distribution axis oriented northeast (Fig. 7). It is likely that the ash cloud flowed down to this point on 23 or 24 May 2003, though Trusdell et al. (2005—this issue) suggested that this event occurred during 28 May–5 June. Ashes in this event were probably minor in volume, since deposits corresponding to gray and brown ashes at this site were not found on top of the dark brown, clast-rich layer inside the caldera or in the eastern part (Figs. 5 and 6).

3.5. Volume and composition of tephra

Tephra volume was estimated based on the isopach maps of Fig. 7 by the method of Fierstein and

Nathenson (1992). Tephra and dense rock densities of 1,400 kg/m^3 and 2,500 kg/m^3 were assumed. We measure the thickness of brown tephra at the rim of the inner crater at 15 m. Though the method of Fierstein and Nathenson (1992) is an empirical one for plinian eruption columns, we used it because the major part of the 2003 eruption products was deposited from the eruption columns of middle May. The total volume of eruption products from the May–June 2003 eruption can be roughly estimated to be 2.58×10^7 m^3; 1.44×10^7 m^3 as DRE; brown tephra of 1.08×10^7 m^3 DRE and gray tephra of 3.7×10^6 m^3 DRE. The total value is close to the volume estimate by Trusdell et al. (2005—this issue) (1.45×10^7 m^3 DRE), who calculated the volume of deposits within the island (on-land deposits), whereas our estimate involves deposits extrapolated to the ocean.

Pumice and volcanic bombs are aphyric andesite. Small amounts ($\leqslant$5 vol.%) of phenocrysts (up to 1 mm long) of plagioclase, clinopyroxene, orthopyroxene and magnetite are included in a glassy or intersertal matrix. Aggregation of phenocrysts is also found. Tiny microlites are abundant in the matrix of bombs while they are scarce in the pumice. Pumice clasts and bombs together with gray ash were analyzed by XRF (PW2400) in ERI, University of Tokyo (Table 1). Lumps of fine gray ash were analyzed as bulk. Lava samples of older lava flows and pyroclastic layers were taken and analyzed in this study for comparison with products of the May–June 2003 eruption (Fig. 9). Pumice samples with different colors and vesicularities are chemically identical (about 61.0–61.3 wt.% SiO_2); differences in color of pumice samples result from their different vesicularity; the lower vesicularity, the darker in color. All bomb samples analyzed are a little poorer in SiO_2 (60.6–60.9 wt.%). Gray ash is chemically variable and more depleted in SiO_2 (60.1–60.7 wt.%). Therefore, the eruption products of the May–June 2003 eruption decrease in SiO_2 with time. Although pumice and bomb samples change chemically together with

Table 1

Type	Pumice		Bomb		Gray ash	
Obs. point no.	104	5	18	106	17	
In wt.% (recalculated the sum of oxides to 100%)						
SiO_2	61.23	61.13	60.71	60.83	60.61	60.41
TiO_2	0.93	0.93	0.94	0.94	0.89	0.86
Al_2O_3	15.60	15.47	15.61	15.49	16.40	16.96
FeO	8.33	8.51	8.61	8.61	8.35	8.75
MnO	0.22	0.23	0.23	0.22	0.20	0.18
MgO	2.10	2.14	2.21	2.21	2.26	2.16
CaO	5.70	5.72	5.89	5.86	5.99	5.71
Na_2O	4.18	4.16	4.15	4.16	3.75	3.50
K_2O	1.42	1.43	1.39	1.40	1.29	1.22
P_2O_5	0.28	0.29	0.28	0.28	0.25	0.26
FeO*/MgO	3.97	3.99	3.90	3.90	3.69	4.06
In ppm						
Ba	399	419	380	374	383	366
Co	20	19	21	22	19	21
Cr	2	4	0	0	6	7
Cu	65	50	61	61	54	80
Nb	4	4	3	3	3	3
Sc	24	26	24	24	27	26
V	115	110	130	131	136	143
Ni	3	0	1	2	5	3
Zn	105	109	106	107	101	95
Rb	28	28	25	25	25	24
Zr	108	108	106	106	101	101
Sr	356	351	361	360	358	364
Y	39	39	39	39	37	36

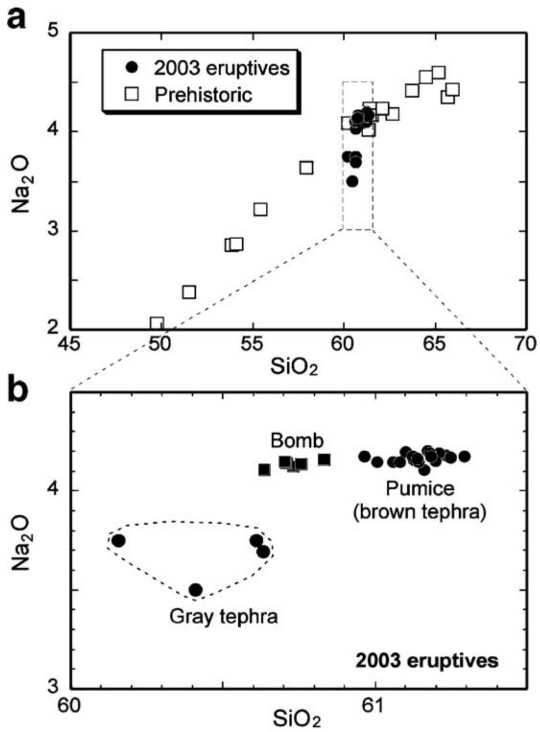

Fig. 9. SiO_2–Na_2O variation diagram of the 2003 eruptives together with prehistoric lavas. All samples were analyzed in this study. Bombs are fragments of the lava dome formed in early June 2003, and accompanied the phreatomagmatic eruptions of gray tephra.

prehistoric lava samples continuously in the Na_2O–SiO_2 variation diagram, gray ash samples are depleted in Na_2O (Fig. 9) and K_2O.

4. Discussion

The dark brown clast-rich ash to lapilli-fall layer that is the topmost deposit in the brown tephra is the thickest single layer near the Eastern Crater. It consists of the largest grains among the layers within the brown tephra. Except for the evidence of partial erosion at Anatahan Village, the layer is stratigraphically continuous on the top of the underlying layers. This implies that the energy of explosions increased with time in the brown tephra, and that deposition of brown tephra was almost continuous. According to BGVN (v. 28, nos. 5 and 6), the eruption cloud had been observed since the evening of 10 May and soon reached 13.4 km. The tremor level remained very high for a couple of days after the first explosion, and the maximum amplitude of volcano-tectonic earthquakes also increased with time over the first two days. Therefore, we can conclude that most of the brown tephra was deposited within a few days following the beginning of the 10 May eruption. Assuming that the tephra was erupted within 30 h based on seismic data (BGVN, v.29, no. 6, pp. 10), the average discharge rate can be calculated as 100 m^3/s (2.5×10^5 kg/s); $2{,}500 \times 1.08 \times 10^7/(30 \times 3{,}600)$. The rate is almost one order of magnitude less than the curve for the discharge rate-maximum column height relationship in plinian explosions modeled by Sparks (1986). According to this relationship, the mass discharge rate of $2–5 \times 10^6$ kg/s is required for the height 13.4 km. The reasons of this discrepancy might come either from underestimation of the tephra volume or from a shorter effective duration of the explosion. However, a phreatomagmatic explosion does not necessarily fit the modeled curve, where the expansion of vapor from an external source may play a major role in sending fine particles to higher levels. For example, the most explosive event at Miyake-jima in 2000 sent an ash cloud as high as 16 km above the volcano, although the discharge rate was as small as 10^6 kg/s (Nakada et al., in press). In this respect, explosions during 10–11 May 2003 may be of phreatomagmatic origin, as suggested by Hilton and Fischer based on their field observations (BVGN v. 28, no. 5).

The gray tephra was the product of phreatomagmatic explosion (base surges), which occurred after about a month of low level eruptive activity following the main explosive phase. Explosive phreatic events following magmatic eruptive phases occurred during the 1790 eruptions at Kilauea by McPhie et al. (1990). The final explosion was the only phreatic event among a series of eruption phases and generated a pyroclastic surge that killed a group of Hawaiian warriors. McPhie et al. (1990) concluded that a subsiding magma column supplied heat for steam production that drove the phreatic explosions. In terms of eruption sequence, the May–June eruption may be similar to the 1790 eruptions at Kilauea. The altitude of the Eastern Crater at Anatahan was 68 m asl before the 10 May 2003 eruption, and it was 10 m below sea level in the middle of June. As the ground-water aquifer level around the crater is expected to be approximately at sea level, magma inside the inner crater should have had a high possibility of meeting water after the eruption of May 2003. It is likely that the resumption of the eruption in the middle of June was caused by interaction of magma with ground water. The lava dome located inside the crater was easily fragmented by explosions derived from magma–water-interaction. Fragments of dome lava could have been discharged outside the Eastern Crater beyond its high walls (as high as 400 m). Fine particles were produced by interaction with water and could have been spilled over the high crater walls. It is expected that the forces of ash-and-steam currents (base surges) by phreatomagmatic explosions were interfered by the high crater walls, so that surges that reached on the caldera floor were not very strong.

Depletion of alkalies in the gray tephra may be caused by their chemical leaching in the hot eruption cloud or after deposition. Experimental data (e.g., Hamilton et al., 2000) showed large dissolution rates of alkalies from natural glass in a strong acid and high temperature solution. As particles of gray tephra are less than 1 mm across even near the Eastern Crater (Fig. 8) and abundant SO_2 and steam was issued during and after the May–June 2003 eruption, chemical leaching would have easily occurred in the vapor-saturated cloud accompanying the phreatomagmatic explosions. Although minor chemical leaching might have operated on the brown tephra, pumices with much larger dimension than particles of gray tephra were analyzed (Table 1).

5. Concluding remarks

(1) At Anatahan Volcano, the most explosive phase during 10–11 May 2003 deposited brown tephra over most of the island. Phreatomagmatic explosions during 14–16 June 2003 sent gray tephra over a more limited area.
(2) Interaction of the magma head with ground water is considered to have generated phreatomagmatic explosions in the middle of June. The lava dome formed in the inner crater in early June was destroyed by these explosions.
(3) A small high-temperature ash-cloud descended to the east during 23–24 May 2003.
(4) Despite the low magma-discharge rate of about 2.5×10^5 kg/s for the 10–11 May eruption, the eruption cloud rose up to 13.4 km. This probably is due to the high explosivity of the eruption related to the involvement of ground water.
(5) Magma of the May–June 2003 eruption was andesite and became slightly depleted in SiO_2 in the order from brown tephra through lava dome material to gray tephra. Alkalies in fine ash particles of the gray tephra may have been chemically leached in the acid hydrothermal fluid during phreatomagmatic explosions.
(6) Though the inner crater had cooled down since the middle of June 2003 eruption, the eruption resumed effusively in April 2004, after about 9 months of quiescence, and scoria and lava began to fill the inner crater. Small strombolian-like explosions occurred repeatedly inside the crater to at least June 2004.

Acknowledgements

Expenses for geological inspection were defrayed from the Grant-in-Aid for Science Research No. 14403003 from the Japan Society for the Promotion of Science, and the 2003 fund of the Disaster Prevention Research Forum, Japan. Grain size analysis of tephra was supported by Mr. M. Nagai. An early version of the manuscript was improved by T. Wright. The manuscript was enhanced by critical reviews by C. Newhall and T. Fischer.

References

Bulletin of Global Volcanism Network (2003 and 2004) Anatahan. Smithsonian National Museum of Natural History 28, no. 4, 2–3; no. 5, 2–5; no. 6, 10–11; 29, no. 4, 7–8.

Fierstein, J., Nathenson, M., 1992. Another look at the calculation of fallout tephra volumes. Bulletin of Volcanology 54, 156–167.

Fujii, T., Nakada, S., 1999. The 15 September 1991 pyroclastic flows at Unzen Volcano (Japan): a flow model for associated ash-cloud surges. Journal of Volcanology and Geothermal Research 89, 159–172.

Hamilton, J.P., Pantano, C.G., Brantley, S.L., 2000. Dissolution of albite glass and crystal. Geochimica et Cosmochimica Acta 64, 2603–2615.

Johnson, P., 2003. Map of EM300 multibeam sonar bathymetry around Anatahan island. Hawaii Mapping Research Group in the site; http://oceanexplorer.noaa.gov/explorations/03fire/logs/anatahan/anatahan.html.

Kato, T., Beavan, J., Matsushima, T., Kotake, Y., Camacho, J.T., Nakao, S., 2003. Geodetic evidence of back-arc spreading in the Mariana Trough. Geophysical Research Letters 30, 1625. doi:10.1029/2002GL016757.

Larson, E.E., Reynolds, R.L., Merrill, R., Levi, S., Ozima, M., Aoki, Y., Kinoshita, H., Zasshu, S., Kawai, N., Nakajima, T., Hirooka, K., 1975. Major-element petrochemistry of some extrusive rocks from the volcanically active Mariana Islands. Bulletin of Volcanology 38, 361–377.

Maruyama, I., 1954. Anatahan. Hermitage House Inc., New York, p. 206.

McPhie, J., Walker, G.P.L., Christiansen, R.L., 1990. Phreatomagmatic and phreatic fall and surge deposits from explosions at Kilauea volcano, Hawaii, 1790 AD: Keanakakoi ash member. Bulletin of Volcanology 52, 334–354.

Nakada, S., Nagai, M., Kaneko, T., Nozawa, A., Suzuki-Kamata, K., in press. Chronology and products of the 2000 eruption of Miyakejima Volcano, Japan. Bulletin of Volcanology.

Rowland, S.K., Lockwood, J.P., 1990. Geology and Volcanic Hazards of Anatahan Volcano, Northern Marianas Islands (abstract). EOS, Transactions American Geophysical Union 71, 1712.

Sako, M.K., Trusdell, F.A., Koyanagi, R.Y., Kojima, G., Moore, R.B., 1995. Volcanic investigations in the Commonwealth of the Northern Mariana islands, April to May 1994. U. S. Geological Survey Open-File Report 94-705, p. 57.

Simkin, T., Howard, K.A., 1970. Caldera collapse in the Galapagos island, 1968. Science 169, 429–437.

Sparks, R.S.J., 1986. The dimensions and dynamics of volcanic eruption columns. Bulletin of Volcanology 48, 3–15.

Tanakadate, H., 1940. Volcanoes in the Mariana Islands in the Japanese mandated south seas. Bulletin of Volcanology 6, 200 – 223.

Trusdell, F.A., Moore, R.B., Sako, M., White, R.A., Koyanagi, S.K., Chong, R., Camacho, J.T., 2005. The 2003 eruption of Anatahan Volcano, Commonwealth of the Northern Mariana Islands: chronology, volcanology, and deformation. Journal of Volcanology and Geothermal Research 146, 184 – 207 (this issue).

Watanabe, T., Tabei, T., Matsushima, T., Kato, T., Nakada, S., Yoshimoto, M., Chong, R., Camacho, J.T., 2005. Geodetic constraints for the mechanism of Anatahan eruption of May 2003. Journal of Volcanology and Geothermal Research 146, 77 – 85 (this issue).

Wiens, S.A., Shore, R.J., Hilton, D., Sauter, A., Hilton, D.R., Fischer, T., Camacho, J.T., 2004. Observing the historic eruption of Northern Mariana Islands Volcano. EOS, Transactions American Geophysical Union 85 (2), 4.

Woodhead, J.D., 1988. The origin of geochemical variations in Mariana Lavas: a general model for petrogenesis in Intra-oceanic Island Arcs? Journal of Petrology 29, 805 – 830.

Wright, T.L., Takahashi, T.J., Griggs, J.D., 1992. Hawai'i Volcano Watch. A Pictorial History, 1779–1991. University of Hawaii Press, p. 162.